ACS Catalysis

Research Article

pubs.acs.org/acscatalysis

Core–Shell-Structured Titanosilicate As A Robust Catalyst for Cyclohexanone Ammoximation

Le Xu, Hong-gen Peng, Kun Zhang, Haihong Wu,* Li Chen, Yueming Liu, and Peng Wu*

Shanghai Key Laboratory of Green Chemistry and Chemical Processes, Department of Chemistry, East China Normal University, North Zhongshan Road 3663, Shanghai 200062, China

Supporting Information

ABSTRACT: Core–shell-structured MWW-type titanosilicate (Ti-MWW) with a well-defined micro-meso hierarchical porosity was fabricated by using self-assembly technique. This composite material Ti-MWW@meso-SiO_2 was applied as the catalyst for the ammoximation of cyclohexanone in a continuous slurry reactor. The combination of characterizations, such as XRD, SEM, HR-TEM, and N_2 adsorption, verified that the composite material was composed of zeolite crystallites as core and mesosilica as shell and that the micropores and mesopores were penetrated well with each other, which significantly facilitated the diffusion of large molecules. In continuous ammoximation of cyclohexanone as a probe reaction, the composite exhibited significantly prolonged lifetime in comparison to the parent Ti-MWW catalyst and the physical mixture of Ti-MWW and mesosilica. The unique catalytic behaviors of Ti-MWW@meso-SiO_2 were ascribed to protecting effect of the mesosilica shell. It served as a sacrificial lamb that protected the active component of zeolite core against rapid desilication and coke formation, leading to a stable duration of the catalysts.

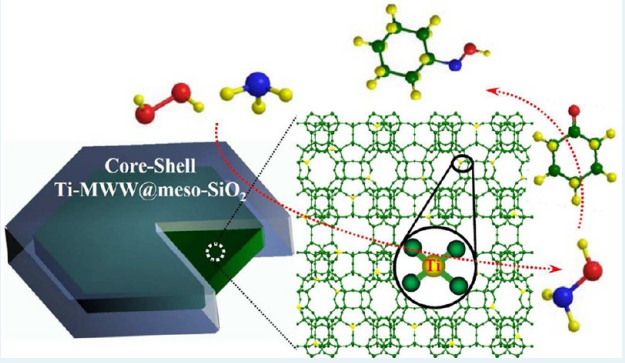

KEYWORDS: *zeolite, titanosilicate, MWW, ammoximation, core–shell structure, cyclohexanone*

1. INTRODUCTION

Zeolites are widely used in oil refining and petrochemical industry as important heterogeneous catalysts. The active sites incorporated in the crystalline framework possess an excellent activity, whereas the micropores with uniform dimensions endow zeolites with a unique shape selectivity for products.[1−6] Thus, zeolites containing either tetrahedral Al or transition metals like Ti have been applied in a variety of processes as solid-acid or oxidation catalysts.[7−11] For instance, using hydrogen peroxide as a clean oxidant, MFI-type titanosilicate (TS-1) is demonstrated to be an effective solid catalyst for a large number of liquid-phase oxidation reactions including epoxidation of olefins, oxidation of alkanes to alcohols and ketones, oxidation of alcohols, hydroxylation of aromatics, oxidation of amines, ammoximation of ketones, and selective oxidation of sulfur-containing compounds and ethers.[12−17] However, the zeolite catalysts are usually employed under severe operating conditions, such as high temperature, acidic or basic systems either in gas-phase or liquid-phase reactors.

Although they exhibit excellent activities as well as rigid physical structures, rigorous reaction environments may deactivate zeolites easily because of coke formation, active site leaching and even framework degradation reaction in specific reaction media. In particular, these factors dominate the liquid-phase ammoximation process of ketones with H_2O_2 and ammonia, an innovative and green reaction developed on the basis of titanosilicate catalyst.[18] In the presence of excessive ammonia with a strong basicity, the titanosilicates are encountered with the deactivation issues fundamentally different from those in conventional reactions over aluminosilicate zeolites. A partial dissolution of silicalite framework was unavoidable under basic condition, which then alters the existing scaffold of Ti active sites. In addition, heavy by-products with high boiling temperature may deposit within zeolite pores to cover the Ti sites, making them inaccessible to reactant molecules. Desilication and coke formation appear to be two key deactivation factors that govern the stability and lifetime of titanosilicates in ammoximation.[19−21] From the point of view of actual applications, it is desirable to develop useful and practical methods that can prolong the catalyst lifetime in the liquid-phase reactions especially conducted in basic media.

In recent years, considerable effort has been devoted to control the fabrication of well-defined core–shell composite materials.[22−28] Core–shell composite materials often exhibit improved properties over the single component and their physical mixture. Particle coating is carried out for different purposes. For example, the shell can alter the charge, functionality, and dispersibility of the core particles. Magnetic, optical, or catalytic crystals could be readily coated to form the

Received: September 12, 2012
Revised: November 26, 2012
Published: November 28, 2012

   dx.doi.org/10.1021/cs3006007 | ACS Catal. 2013, 3, 103−110

composite materials with different properties. Encasing colloids in a shell with different composition may also protect the core from extraneous chemical and physical changes. Somorjai et al reported the synthesis of a high-temperature-stable core−shell catalyst, Pt@mSiO$_2$,[29] in which the silica shell protected the Pt nanoparticles cores from deformation and aggregation. Therefore, the core−shell catalyst stood up to 750 °C in air for ethylene hydrogenation and CO oxidation. The magnetic particles, on the other hand, were also coated with the mesoporous silica shell.[30−33] The core−shell magnetic mesoporous silica microspheres possessed strong magnetic responsivity, orientated and accessible mesopores and high dispersibility. In the case of zeolite core, TS-1 and ZSM-5 zeolites have been coated with mesoporous silica shell by using cationic or nonionic surfactants as porogen, giving rise to the mesosilica shell with different mesoporosities.[34−37] These zeolite-based core−shell materials can serve as multifunctional catalysts. The introduction of the mesoporous shell provides the scaffolds for constructing other catalytic sites, or protects the zeolite crystals from chemical and physical changes in catalytic reactions.

Titanosilicate with the MWW topology, Ti-MWW, has been shown to be effective to the ammoximation of cyclohexanone, an important reaction for nylon 6 synthesis. In the batchwise reactor, Ti-MWW was capable of giving both cyclohexanone conversion and oxime selectivity over 99% under optimum reaction conditions.[38] In the continuous slurry reactor, Ti-MWW was extremely robust and showed a longer lifetime than other titanosilicates, such as TS-1.[39] However, Ti-MWW suffered deactivation because of desilication and deposition of by-products.

In this study, choosing Ti-MWW as a representative titanosilicate, we propose a strategy for designing and synthesizing robust catalysts useful to selective oxidations in liquid-phase. Through coating mesoporous silica shell over zeolite crystallites via the sol−gel self-assembling route, the novel composite catalyst thus prepared showed a greatly prolonged catalytic lifetime for the ammoximation of cyclohexanone in a continuous slurry reactor. The mesosilica shell serves as a sacrificial lamb that protects the active component of zeolite core against desilication and coke formation, leading to a more robust oxidation catalyst.

2. EXPERIMENTAL SECTION

2.1. Synthesis of Ti-MWW. Following the procedures reported previously,[40,41] Ti-MWW lamellar was synthesized in boric acid system with piperidine (PI) as a structure-directing agent (SDA). The gel with a molar composition of 1.0 SiO_2/0.67 B_2O_3/0.05 TiO_2/1.4 PI/19 H_2O was crystallized at 443 K for 7 days, giving rise to lamellar precursor of Ti-MWW. The precursor was refluxed with 2 M HNO_3 at a solid to liquid weight ratio of 1:50 to remove the extraframework Ti species. The sample was calcined in air at 773 K for 10 h to obtain the Ti-MWW catalyst which had a Si/Ti ratio of 35.

2.2. Preparation of Ti-MWW@meso-SiO$_2$ Core/Shell Materials. Following the procedure adopted previously for synthesizing core/shell-structured Fe_3O_4/mesosilica or TS-1@meso-SiO_2,[30,34] Ti-MWW (4.5 g) was dispersed in a solution containing cetyltrimethylammonium bromide (CTAB) (4.5 g), deionized water (1200 mL), ammonia aqueous solution (15 g, 28 wt %) and ethanol (900 mL). The mixture was subjected to ultrasonic treatment for 0.5 h to from a uniform suspension. Then, a desirable amount of tetraethyl orthosilicate (TEOS) (0.9−7.875 g) was added dropwise to the mixture under continuous stirring. After the reaction at 303 K for 6 h, the product was collected by centrifugation and washed repeated with ethanol and water. To further improve the quality of mesosilica shell, the as-synthesized core−shell samples were hydrothermally treated in water at 403 K for 18 h.[42] Then, the sample was calcined at 823 K for 10 h to remove the organic species occluded, resulting in Ti-MWW@meso-SiO_2 catalyst, denoted as MS.

2.3. Characterization Methods. The X-ray diffraction (XRD) patterns were collected on a Rigaku Ultima IV X-ray diffractometer using Cu−Kα radiation (λ=1.5405 Å). Nitrogen adsorption isotherms were recorded at 77 K on a BELSORP-MAX instrument after activating the fresh sample at 573 K or the deactivated samples at 393 K under vacuum for at least 10 h. The pore size distribution was calculated for mesopores with BJH method and for micropores with Horvath-Kawazoe (HK) method. The SEM images were taken on a Hitachi S-4800 microscope, while the TEM images were taken on a JEOL-JEM-2100 microscope. The amount of Si and Ti was quantified by inductively coupled plasma (ICP) on a Thermo IRIS Intrepid II XSP atomic emission spectrometer. The thermogravimetric and differential thermal analyses (TG-DTA) were performed on a METTLER TOLEDO TGA/SDTA851^e apparatus from room temperature to 1073 K at a heating rate of 10 K min^{-1} in air. UV−visible spectra were recorded on a PerkinElmer Lambda 35 UV−vis spectrometer. The side-products formed during the cyclohexanone ammoximation were determined by using authentic chemicals on a GC-MS (Agilent 6890 series GC system, 5937 network mass selective detector).

2.4. Catalytic Oxidation Reactions. The liquid-phase epoxidation of 1-hexene with hydrogen peroxide was carried out in a batchwise reactor.[43] The mixture containing 50 mg of catalyst, 10 mL of MeCN, 10 mmol of 1-hexene, and 10 mmol of H_2O_2 (30 wt %) aqueous solution was stirred vigorously at 333 K for 2 h. After the catalyst powder was removed, the products for the reaction were analyzed on a gas chromatograph (Shimadzu 2014, FID detector) equipped with a 30 m DB-WAX capillary column.

The liquid-phase ammoxidation of cyclohexanone was carried out continuously in a 160 mL glass slurry reactor equipped with a glass sand filter and a magnetic stirrer.[39] For a typical reaction, a desired amount of catalyst (1.0−2.86 g) and 110 mL of *tert*-butanol aqueous solution (85 wt.%) were added in the reactor and heated under stirring at 344 K. The mixture solution of cyclohexanone and 85 wt.% *t*-BuOH solution and 27.5 wt.% H_2O_2 aqueous solution were then fed into the reactor separately with micro-pumps. The feeding rate of the mixture of cyclohexanone and *t*-BuOH was always kept constant at 96 mL h^{-1}. Meanwhile, ammonia gas (99.9%) was charged into the reaction system with a mass flowmeter at a constant rate. The molar ratios of H_2O_2/ketone and NH_3/ketone were 1.1 and 1.7, respectively. With the reaction proceeding, the reaction mixture overflowed from the outlet filter and the catalyst remained in the reactor. The ammonia unconverted and not soluble in the reaction solution was exhausted through a condenser vent. The organic products were analyzed on a gas chromatograph (Shimadzu 14B) with a flame ionization detector and a HP-5 capillary column to calculate the conversion of cyclohexanone and the selectivity of oxime. The deactivated catalysts were filtered, washed using 50

dx.doi.org/10.1021/cs3006007 | ACS Catal. 2013, 3, 103−110

mL of H_2O, dried at 323 K. The deactivated catalysts were regenerated by calcination at 823 K in air.

3. RESULTS AND DISCUSSION

3.1. Preparation and Characterizations of Ti-MWW@meso-SiO_2.

Ti-MWW@meso-SiO_2 (denoted as MS) with a core−shell structure was prepared through a self-assembly approach.[30,34,35] Ti-MWW was first hydrothermally synthesized followed by acid washing and calcination.[40,41] Then it was dispersed in the mixture of H_2O, ethanol, ammonia, and CTAB, which was very similar to the Stöber method.[44] The concentration of surfactant was very low in the solution, avoiding a too rapid self-assembly of mesosilica in phase separation manner. The mixture was subjected to ultrasonic treatment to make the zeolite particles highly dispersed as possible. The addition of TEOS under vigorous stirring induced the assembly of mesosilica covering the zeolite particles, leading to as-synthesized core−shell composite. The obtained powder was further hydrothermally aged in water at 403 K for 18 h, which enhanced the condensation and mesopore array order of the mesosilica shell.[42] The materials were calcined in air to remove any occluded organic species.

The field-emission scanning electron microscopy (FE-SEM) images depict the realization of constructing mesoporous silica shell on the surface of Ti-MWW core. Ti-MWW was composed of pellet like crystallites with a relatively smooth surface (Figure 1a). After subjected to ammonia-assisted sol-gel coating in dilute solution of TEOS and CTAB, the original pellet morphology of Ti-MWW was almost preserved, but the crystallites showed a roughness on the surface and an enlarged thickness of the pellets (Figure 1b−g). This phenomenon was observed clearly when changing the TEOS/Ti-MWW weight ratio. When the ratio was increased from 0.2 to 1.5, the resultant materials increased in particle size systematically. These results imply that the assembly of mesosilica phase took place controllably on the surface of Ti-MWW crystallites, which was essentially similar to the previous synthesis when using TS-1[34] or ZSM-5[35] as the core materials. However, the phase separation occurred when the TEOS/Ti-MWW mass ratio reached 1.75. In addition to core−shell crystallites, the microspheres co-existed because of that the redundant silica species were self-assembled independently in a phase manner, forming MCM-41-like mesoporous silica (Figure 1h). Therefore, the TEOS/Ti-MWW mass ratio should be controlled below 1.5 to obtain well-defined core−shell materials.

The transmission electron microscopy (TEM) images further confirmed the core−shell structure with Ti-MWW crystallite as a core and mesosilica as a shell was really constructed (Figure 2).The low resolution TEM image shows the composite possessed a uniform core−shell structure (Figure 2a and b). The high resolution TEM (HR-TEM) images taken along [100] and [001] incidences indicated that the meso-channels lacked somewhat order array in the shell part, but they were accessible with pore entrances open to outside. The different crystalline planes of the MWW framework were clearly observable from both images (Figure 2c and d). The meso-channels templated by CTAB were perpendicular to the zeolite core, which may be advantageous the diffusion of the reagent molecules in actual catalytic reactions. The thickness of mesoporous silica shell was about 30−40 nm from [100] direction and about 15−20 nm from [001] direction at TEOS/Ti-MWW weight ratio of 1.5. The crystallite surface of Ti-MWW was deprotonated in the basic medium, leading to a negatively charged surface. A strong interaction then occurred between the deprotonated Si−O^- and positively charged

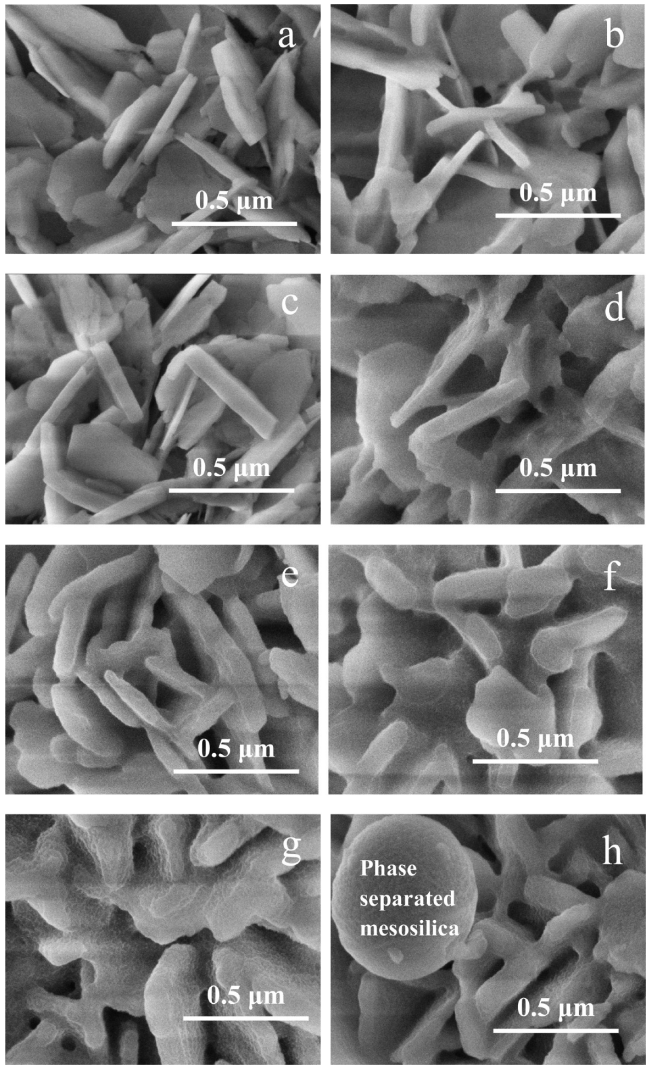

Figure 1. SEM images of Ti-MWW (a) and Ti-MWW@meso-SiO_2 prepared at a TEOS/Ti-MWW weight ratio of 0.2 (b), 0.5 (c), 1.0 (d), 1.15 (e), 1.25 (f), 1.50 (g), and 1.75 (h).

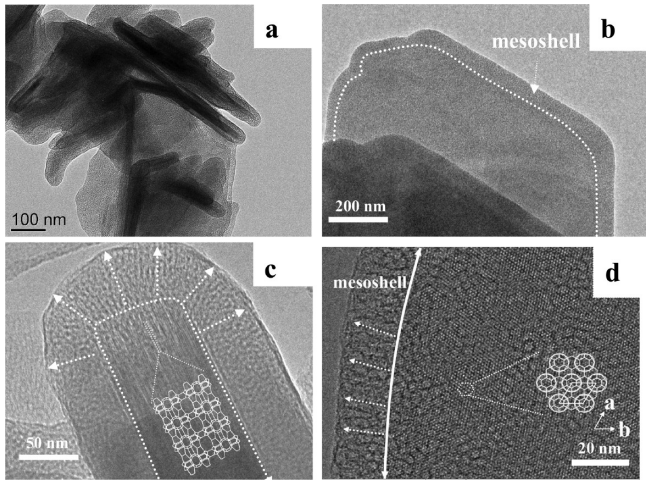

Figure 2. HR-TEM images of Ti-MWW@meso-SiO_2-1.5TEOS taken along the directions of [100] (a, c) and [001] (b, d).

dx.doi.org/10.1021/cs3006007 | ACS Catal. 2013, 3, 103−110

cationic surfactant micelles, which made the crystallite surface rich in CTAB. The silicate oligomers from TEOS hydrolysis then interacted with CTAB attached on the crystallite surface to bring about a coating and assembly process around the zeolite.

The MS materials showed a broad XRD diffraction at 2θ of 2.6° in low-angle range, which was absent for Ti-MWW (Figure 3). The patterns lacked the diffractions with higher plane

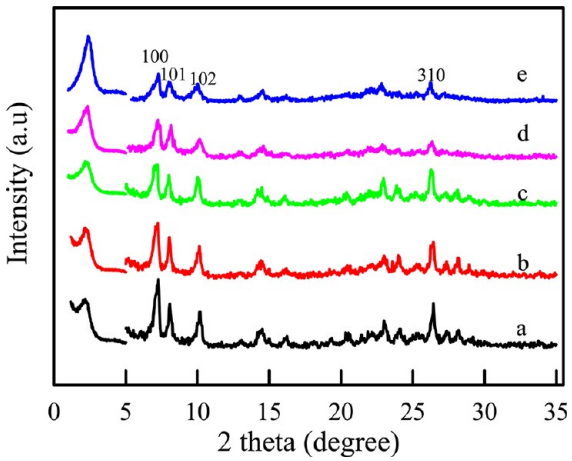

Figure 3. XRD patterns of Ti-MWW@meso-SiO_2 prepared at a TEOS/Ti-MWW weight ratio of 0.5 (a), 1.0 (b), 1.25 (c), 1.5 (d), and at 1.5 after aging process (e).

indexes usually observed for ordered mesosilica, such as MCM-41 and SBA-15, suggesting that the shell may possess a wormhole-like mesopores. The intensity of this reflection slightly increased with increasing shell thickness. In high-angle region, the diffractions duo to the MWW topology remained, and reasonably decreased in intensity after coated with amorphous mesosilica shell. The mild coating conditions did not influence the structure of zeolite core. A subsequent hydrothermal treatment further enhanced the intensity of this reflection, indicating the quality and structure order of the mesosilica shell were improved (Figure 3e). However, the intensity of diffractions due to MWW structure in high-angle region decreased to some extent after aging process (Figure 3e). These results suggested that the defect sites within MWW structure were probably attacked by H_2O molecules during hydrothermal aging process, which caused the MWW structure to degrade partially. To investigate the influence of hydrothermal treatment on the catalytic performance of the Ti-MWW core, we have investigated the catalytic behavior of MS-1.5TEOS before and after aging process in the ammoximation of cyclohexanone. As shown in Supporting Information Table S1, MS-1.5TEOS showed very comparable cyclohexanone conversion irrespective of aging or not. This indicated that the aging process did not make negative impact on the catalytic properties of Ti-MWW core.

Figure 4 compares the N_2 adsorption isotherms of parent Ti-MWW and MS with different shell thickness. Ti-MWW exhibited a typical type I adsorption isotherm characteristic of microporous materials, whereas MS displayed an isotherm with a capillary condensation at P/P_0 of 0.2 - 0.4, which was due to multilayer adsorption of nitrogen in mesopores.[45,46] As the shell thickness increased, the type of isotherms changed from type I to type IV gradually. The textural properties related to mesoporosity closely depended on the amount of TEOS added (Table 1). The specific surface area, total pore volume and

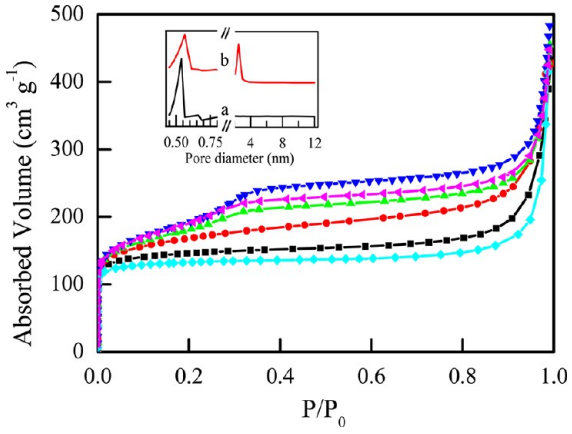

Figure 4. N_2 adsorption and desorption isotherms and of Ti-MWW and MS prepared at TEOS/Ti-MWW weight ratio of 0.5, 1.0, 1.25, 1.5, and at 1.5 after aging process (from bottom to upper). The inserts shows the pore size distribution of Ti-MWW (a) and Ti-MWW@meso-SiO_2-1.5TEOS (b).

Table 1. Physicochemical Properties of Ti-MWW and Ti-MWW@meso-SiO_2 (MS) at Different TEOS/Ti-MWW Mass Ratio

			pore volume (cm^3 g^{-1})		
sample	Si/Ti[a]	SSA[b] (m^2 g^{-1})	total	mesopores	micropores[c]
Ti-MWW	35	534	0.204	0.013	0.191
MS-0.5TEOS	39	571	0.228	0.043	0.185
MS-1.0TEOS	42	599	0.279	0.105	0.174
MS-1.25TEOS	46	624	0.298	0.130	0.168
MS-1.5TEOS	49	657	0.338	0.178	0.160
MS-1.5TEOS[d]	49	672	0.350	0.186	0.164

[a]Determined by ICP analysis. [b]SSA, specific surface area calculated by BET method from N_2 adsorption isotherms at 77 K. [c]Calculated by *t*-plot method. [d]After aging process.

mesopore volume increased with the mesosilica shell thickness, while the micropore volume decreased reasonably. The inset in Figure 4 shows the pore size distribution of Ti-MWW together that of a representative MS material, Ti-MWW@meso-SiO_2-1.5TEOS. Ti-MWW contained only micropores of 0.54 nm, corresponding to the 10-MR channels of MWW structure,[47] while MS possessed an additional narrow distribution peak at 2.1 nm due to the mesopores in the shell part. In agreement with above HR-TEM images, the N_2 adsorption verified that the micropores in zeolite core were interconnected with the shell mesopores. UV-visible spectra showed that the active Ti sites remained tetrahedrally coordinated, showing a characteristic band at 210 nm (Figure 5), indicating that the coating process did not alter the state and coordination of the active Ti sites. The Si/Ti ratio increased from 35 in Ti-MWW to 49 in MS at TEOS/Ti-MWW weight ratio of 1.5 (Table 1), implying the loading of Ti-MWW in this hybrid material was about 70 wt. % if the Ti species were intact in coating process.

We have further checked whether the Ti-MWW active component covered with mesosilica shell was really accessible in actual catalytic reactions. The parent Ti-MWW and MS-1.5TEOS have been employed as catalysts in the epoxidation of 1-hexene with H_2O_2 (Table 2). Ti-MWW showed higher conversion than corresponding MS-1.5TEOS catalyst when the reactions were carried out at the same catalyst loading. With

dx.doi.org/10.1021/cs3006007 | ACS Catal. 2013, 3, 103−110

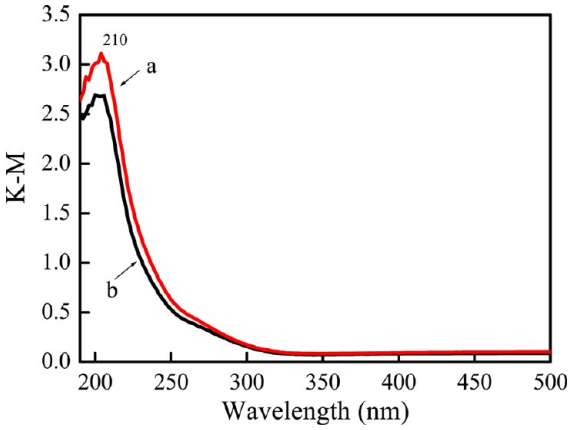

Figure 5. UV−visible spectra of Ti-MWW (a) and Ti-MWW@meso-SiO_2-1.5TEOS (b).

Table 2. Comparison of Liquid-Phase Epoxidation of 1-Hexene with H_2O_2 between Ti-MWW and MS-1.5TEOS[a]

cat.	Si/Ti[b]	1-hexene conv. (%)	epoxide sel. (%)	TON (mol (mol-Ti)$^{-1}$)	H_2O_2 eff. (%)
Ti-MWW	35	55.3	99.1	236	93.2
MS-1.5TEOS	49	40.7	99.3	241	92.8

[a]Reaction conditions: cat., 50 mg; 1-hexene, 10 mmol; H_2O_2 (30 wt. %), 10 mmol; MeCN, 10 mL; temp., 333 K; time, 2 h. [b]Determined by ICP analysis.

respect to the specific activity per Ti site, that is, turnover number (TON), the two catalysts were comparably active, indicating the Ti sites existing in the titanosilicate core of core/shell-structured material were accessible to both 1-hexene and H_2O_2. The H_2O_2 efficiency was over 90%. Even under the reaction conditions that H_2O_2 used was 10 times as much as 1-hexene, the H_2O_2 efficiency still reached 90%. These results strongly suggested that the micropores and mesopores were well interconnected. Considering the fact that the dimension of the shell mesopores (2.1 nm) were about four times that of the core micropores (0.54 nm) and the mesopores were almost perpendicular to the zeolite crystal surface, these two kinds of pores would have a high interconnecting probability on the boundary. Thus, the MS materials with a multi-pore structure can be employed as catalysts for ammoximation reactions.

3.2. Catalytic Properties of Ti-MWW@meso-SiO_2-1.5TEOS in Continuous Ammoximation of Cyclohexanone in a Slurry Reactor. Simulating the operating conditions in industrial processes, we carried out the ammoximation of cyclohexanone with H_2O_2 and NH_3 in a continuous slurry reactor as reported previously.[39] This is a rapid deactivation system which can evaluate the catalytic properties of titanosilicates within a relatively short time. Generally, the ammoximation reactions prefer a basic environment created by an excess of NH_3.[48] The reactions were carried out at the NH_3/cyclohexanone molar ratio of 1.7, higher than the stoichiometric ratio of 1. The excessive NH_3 partially evaporated or dissolved in the liquid-phase of the reaction mixture. On the other hand, the H_2O_2/cyclohexanone molar ratio was maintained at 1.1 which was only slightly higher than the stoichiometric ratio, considering that a part of H_2O_2 may undergo unproductive decomposition. The reaction parameters have been optimized by investigating the effects of various reaction conditions in particular the reaction temperature. At 343 K, the cyclohexanone conversion and corresponding oxime selectivity reached >96 % and >99.5 %, respectively. When the catalyst began to deactivate, the conversion dropped sharply to 50 % within 2 h. The time point when the cyclohexanone conversion decreased below 95% was defined as the lifetime of the catalysts. Figure 6 shows typical time course at the same

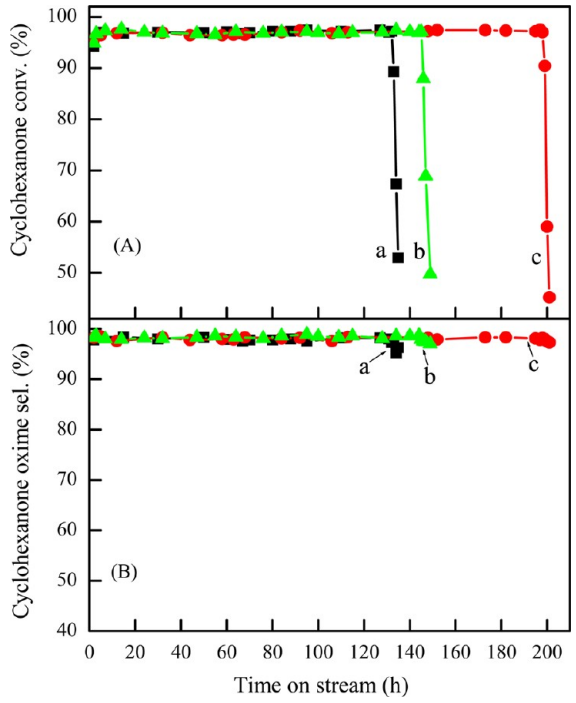

Figure 6. Cyclohexanone conversion (A) and cyclohexanone oxime selectivity (B) in the ammoximation on Ti-MWW (a), physical mixture of Ti-MWW (70 wt.%) and mesosilica (30 wt.%) (b) and Ti-MWW@meso-SiO_2-1.5TEOS (c) at the same loading of Ti-MWW active component (2.0 g).

loading of Ti-MWW active component (2 g), whereas the results using different catalyst weight are listed in Table 3. As already known, the ammoximation lifetime and the amount of processed cyclohexanone depend closely on the titanosilicate loading.[39] When the amount of Ti-MWW was varied from 1.0 g to 2.0 g, the ammoximation lifetime was prolonged from 10 to 132 h (Table 3, nos. 2−5). However, the MS-1.5TEOS catalyst exhibited a much longer lifetime than parent Ti-MWW when compared at the same amount of the Ti-MWW active component. The ammoximation lifetime of MS-1.5TEOS was prolonged from 34 h to 198 h with the catalyst loading increasing from 1.0 g to 2.0 g. The MS-1.5TEOS showed lifetime of 34 h, almost three times as long as Ti-MWW catalyst under the same reaction conditions (Table 3, No 2 and 7). When the reactions were carried out using 2.0 g of active zeolite component, MS-1.5TEOS deactivated at 198 h in comparison to 132 h for Ti-MWW (Figure 6 and Table 3, Nos. 5, 10). Obviously, MS-1.5TEOS was more robust against deactivation and superior to Ti-MWW in terms of lifetime.

The causes of deactivation were elucidated to be the coke deposition and partial dissolution of the zeolite framework.[39,49] To clarify the possible reasons for the prolonged lifetime of MS-1.5TEOS, we have analyzed the physicochemical properties of the deactivated catalysts from the above two aspects (Table 3).

dx.doi.org/10.1021/cs3006007 | ACS Catal. 2013, 3, 103−110

Table 3. Textural and Catalytic Properties of Ti-MWW and MS-1.5TEOS

no.	cat.	amount[a] (g)	lifetime (h)	Si/Ti[c]	SSA[d] (m^2 g^{-1})	PV[e] (cm^3 g^{-1})	relative cryst.[f] (%)	weight loss[g] (%)
1	Ti-MWW[b]	–	–	35	534	0.19	100	–
2	Ti-MWW	1.0	10	31	515	0.17	49.6	6.2
3	Ti-MWW	1.2	20	29	414	0.15	44.2	7.2
4	Ti-MWW	1.4	69	23	157	0.13	23.6	18.8
5	Ti-MWW	2.0	132	18	132	0.12	18.4	24.9
6	MS[b]	–	–	49	672	0.16	100	–
7	MS	1.43(1.0)	34	43	301	0.10	69.2	9.7
8	MS	1.71(1.2)	75	40	292	0.09	43.7	10.8
9	MS	2.00(1.4)	127	36	287	0.02	36.1	12.1
10	MS	2.86(2.0)	198	32	268	0.01	30.3	15.9

[a]The number in parentheses indicates the amount of Ti-MWW active component used. [b]Fresh sample (MS: MS-1.5TEOS). [c]Obtained by ICP analysis. [d]SSA, specific surface area (BET). [e]Micropore volume calculated by *t*-plot method. [f]Measured by accumulated intensity of the main XRD diffractions of [100], [101], [310]. The relative crystallinity of the fresh catalyst is assumed to be 100 %. [g]Obtained by TG measurement on deactivated catalysts without calcination.

Firstly, the catalyst was always immersed in a basic solution with the presence of excessive NH_3 (NH_3/cyclohexanone ratio of 1.7). This would make a partial dissolution of zeolite framework unavoidable. Therefore, the crystallinity of used catalysts was decreased gradually during the reaction process. The apparent Si/Ti ratio decreased from 35 to 18 after Ti-MWW was spent for 132 h, whereas that of MS-1.5TEOS decreased from 49 to 32 after the use for 192 h (Table 3). The increase of relative Ti content after reaction indicated that the desilication really occurred. However, the desilication degree of Ti-MWW seems to be more serious than that of MS-1.5TEOS. The XRD patterns were measured to investigate the desilication degree of the deactivated catalysts quantitatively (Supporting Information Figure S1 and S2). The crystallinity of the used catalysts were measured by accumulated intensity of the main diffractions of [100], [101], and [310] in the XRD patterns. The relative crystallinity of the fresh catalyst is assumed to be 100 %. Although the deactivated samples still possessed the typical MWW structure, their crystallinity decreased obviously. The relative crystallinity of Ti-MWW decreased to 18.4 % after being used for 132 h whereas that of MS-1.5TEOS decreased to 30.3 % at 198 h (Table 3, Nos. 5, 10). Notably, the desilication degree of Ti-MWW was more serious than that of MS when compared at the same amount of active component (Figure 7). This revealed that the mesosilica shell existing as an outer shell in MS may be dissolved in advance to Ti-MWW core. Serving as sacrificial lamb, the shell protected the Ti-MWW crystallites from desilication effectively at least at the early stage of ammoximation. The protecting effect of the mesosilica shell thus made the MWW structure more stable in the MS catalysts. As shown in our previous report,[39] the addition of a small amount of silica gel to the reaction system could postponed the deactivation of Ti-MWW effectively, and then prolong the ammoximation lifetime. Obviously, the dissolution of the framework was restricted by the additional silica source. In a control experiment, a physical mixture of Ti-MWW (70 wt.%) and mesoporous silica (30 wt.%), denoted as M&S, was also applied to the continuous ammoximation of cyclohexanone. At the same loading of Ti-MWW (2.0 g), M&S showed a very similar cyclohexanone conversion and oxime selectivity to the parent Ti-MWW (Figure 6). However, the lifetime of M&S was only slightly longer than Ti-MWW, but much shorter than MS. This indicates that the added mesoporous silica could not protect the active component from deactivation as effective as the mesoporous silica shell. In other words, the silica attached to the Ti-MWW surface could play the role in protection the catalysts from desilication much better than the additional silica source. Because of the presence of mesosilica shell, the active center located in the zeolite framework could be protected in the basic reaction solution.

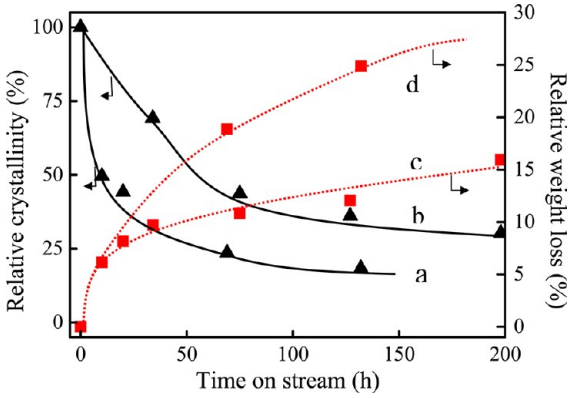

Figure 7. Relative crystallinity and weight loss of deactivated Ti-MWW catalyst (a, d) and deactivated MS-1.5TEOS (b, c) as reaction time in the ammoximation of cyclohexanone.

UV−visible spectra were recorded to check the state and coordination of the Ti active site in the deactivated and regenerated samples. The deactivated Ti-MWW sample showed the adsorptions in the region about 260 nm and 330 nm in addition to the main band at 210 nm (Figure 8a). This implies the deactivated sample contained the Ti species with six-coordination and in non-framework position. These adsorptions decreased in intensity to some extent, but did not disappear after the deactivated sample was regenerated (Figure 8b). In contrast to Ti-MWW, the deactivated MS sample exhibited less obvious adsorptions at 260 or 330 nm (Figure 8c). After regeneration, the spectrum was almost the same as the fresh MS-1.5TEOS sample (Figure 8d). Therefore, the active Ti sites inside zeolite core got well protected by the presence of mesosilica shell in basic reaction media.

In addition to the desilication, coke formation was another key factor accounting for catalytic deactivation.[39] In addition to the main product of cyclohexanone oxime at a selectivity over 99%, the ammoximation also produced several organic byproducts with high boiling temperatures. These byproduct molecules were accumulated and deposited gradually inside the zeolite, blocking the channels and the covering the Ti sites

dx.doi.org/10.1021/cs3006007 | ACS Catal. 2013, 3, 103−110

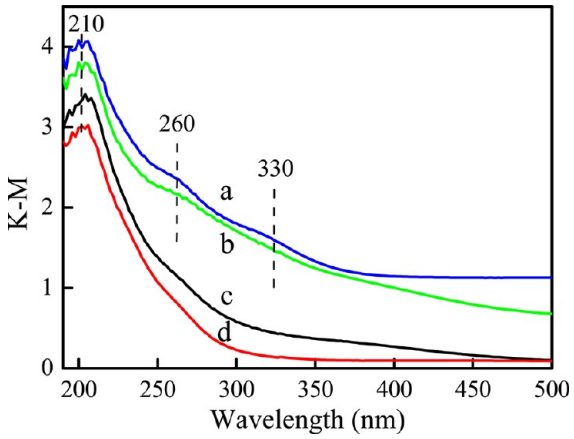

Figure 8. UV−visible spectra of the deactivated and regenerated Ti-MWW (a, b) and MS-1.5TEOS (c, d). Ammoximation condition: Ti-MWW, 1.4 g; others, see Experimental Section.

severely. The N_2 adsorption was carried out to investigate the textural property change in the deactivated catalysts. As shown in Table 3, in comparison to fresh ones, the surface area and pore volume decreased greatly for both deactivated Ti-MWW and MS-1.5TEOS without calcination. This is mainly because of pore blocking by heavy byproducts and coke formation. The deactivated catalyst was extracted in EtOH/HCl solution. Several by-products were qualitatively determined in the extraction by GC-MS analysis (Table 4). They corresponded

Table 4. Major Components of Soluble Organic Byproducts Extracted from Deactivated Catalysts[a]

No.	Molecular weight	Compound	Formula
1	100	Cyclohexanol	
2	113	ε-Caprolactam	
3	127	Cyclohexanecarboxamide	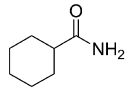
4	179	*N*-Cyclohexylidenecyclohexanamine	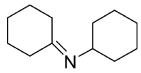
5	180	2-Cyclohexylcyclohexanone	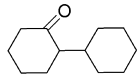
6	187	2-(*tert*-Butylperoxy)-cyclohexanamine	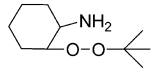

[a]Determined by GC-MS.

to the coke with higher boiling-points than cyclohexanone oxime. TG-DTA profiles were recorded to measure the amount of deposited coke. The weight loss at >473 K was due to coke. It increased with the ammoximation lifetime, as a result of gradual deposition of organic by-products with high molecular weights (Table 3 and Supporting Information Figure S3). Interestingly, the coke deposition rate in deactivated MS increased more slowly in comparison to deactivated Ti-MWW, while the absolute amount of coke deposited on MS was also less than that on Ti-MWW. The coke deposition of MS-1.5TEOS deactivated at 198 h was 15.9 wt.%, while that of deactivated Ti-MWW was 24.9 wt.% irrespective of a shorter lifetime of 132 h (Table 3, nos. 5, 10). According to ammoximation mechanism,[50,51] hydroxylamine is in situ formed inside the titanosilicate pores first. This intermediate subsequently diffuses out of the crystallites pores and interacts with ketone to produce oxime via a non-catalytic oximation route. Because the hydrophilic of the amorphous silica shell and the effect of spatially confinement, the existence of mesosilica shell in MS-1.5TEOS may decrease the concentration of cyclohexanone at the pore entrance of the core catalyst to certain extent. Thereafter, more coke may be formed inside the mesosilica shell or outside the core−shell catalyst. With prolonging processing time, the mesosilica shell was gradually dissolved into the reaction solution as evidenced by the SEM investigation (Supporting Information Figure S4). The coke deposited in the mesosilica then would be taken away simultaneously, which possibly lowered the coke deposition of MS-1.5TEOS in comparison to Ti-MWW.

We further checked the catalytic performance of fresh and regenerated catalysts of Ti-MWW and MS-1.5TEOS. As shown in Supporting Information Table S2, when the reactions were carried out at the same catalyst loading, the Ti-MWW-fresh sample showed a higher cyclohexanone conversion (91.8%) than the MS-1.5TEOS-fresh (71.2%) since the later contained a part of non-active mesosilica. In terms of specific activity, i.e. turnover number (TON), the core−shell material was more active. After the deactivated samples were regenerated and reused in the ammoximation of cyclohexanone, they both showed decreased cyclohexanone conversion and TON in comparison to corresponding fresh ones, mostly because the desilication occurred during reaction. However, MS-1.5TEOS-regenerated showed a higer TON than Ti-MWW-regenerated although the former was spent in the basic reaction mixture for a much longer time (127 h). These results clearly indicated that the core−shell structure was of benefit to lifetime improvement of the catalysts.

4. CONCLUSIONS

In this work, a more robust and catalytically stable core−shell structured titanosilicate catalyst than parent Ti-MWW has been prepared. We have explored the catalytic properties of the novel core−shell catalyst in the ammoximation of cyclohexanone. The catalyst display significantly prolonged lifetime in comparison to parent Ti-MWW and the physical mixture of Ti-MWW and mesosilica. The mesosilica shell is sacrificed in basic reaction media at elevated temperatures, which prevents the active component from desilicating and pore blocking by heavy by-products, and then prolongs the lifetime of the catalyst significantly. This would provide a facile method for designing and synthesizing robust and durable zeolite catalysts useful in the continuous slurry reactors.

■ ASSOCIATED CONTENT

Supporting Information

Figures showing XRD patterns, TG analysis, and SEM images and tables of liquid-phase ammoximation data. This information is available free of charge via the Internet at http://pubs.acs.org/.

■ AUTHOR INFORMATION

Corresponding Author

*E-mail: pwu@chem.ecnu.edu.cn (P.W.); hhwu@chem.ecnu.edu.cn (H.W.).

Notes

The authors declare no competing financial interest.

■ ACKNOWLEDGMENTS

This project was supported by the National Science Foundation of China (20973064, 20925310, U1162102), Ministry of Science and Technology (2012BAE05B02), STCSM (12JC1403600), Shanghai Municipal Education Commission (13zz038) and Shanghai Leading Academic Discipline Project (B409).

■ REFERENCES

(1) Corma, A. *Chem. Rev.* **1997**, *97*, 2373.
(2) Davis, M. E. *Nature* **2002**, *417*, 813.
(3) Wight, A. P.; Davis, M. E. *Chem. Rev.* **2002**, *102*, 3589.
(4) Corma, A. *J. Catal.* **2003**, *216*, 298.
(5) Tao, Y.; Kanoh, H.; Abrams, L.; Kaneko, K. *Chem. Rev.* **2006**, *106*, 896.
(6) Smit, B.; Maesen, T. L. M. *Chem. Rev.* **2008**, *108*, 4125.
(7) Zones, S. I. *Microporous Mesoporous Mater.* **2011**, *144*, 1.
(8) Corma, A.; Serra, J. M. *Catal. Today* **2005**, *107*, 3.
(9) Čejka, J.; Centi, G.; Perez-Pariente, J.; Roth, W. J. *Catal. Today* **2012**, *179*, 2.
(10) Climent, M. J.; Corma, A.; Iborra, S. *Chem. Rev.* **2011**, *111*, 1072.
(11) Rahimi, N.; Karimzadeh, R. *Appl. Catal. A* **2011**, *398*, 1.
(12) Tatsumi, T.; Nakamura, M.; Negishi, S.; Tominaga, H. *Chem. Commun.* **1990**, 476.
(13) Notari, B. *Adv. Catal.* **1996**, *41*, 253.
(14) Clerici, M. G.; Ingallina, P. *J. Catal.* **1993**, *140*, 71.
(15) Bellussi, G.; Rigutto, M. S. *Stud. Surf. Sci. Catal.* **1994**, *85*, 177.
(16) Ratnasamy, P.; Srinivas, D.; Knözinger, H. *Adv. Catal.* **2004**, *48*, 1.
(17) Bhaumik, A.; Kumar, R. *J. Chem. Soc. Chem. Commun.* **1995**, 349.
(18) Ichihashi, H. *Catalysts Catal.* **2005**, *47*, 190.
(19) Roffia, P.; Padovan, M.; Moretti, E.; De Alberti, G. U. S. Patent 4745221, 1988.
(20) Roffia, P.; Padovan, M.; Leofanti, G.; Mantegazza, M. A.; De Alberti, G.; Tauszik, G. R. U. S. Patent 4794 198, 1988.
(21) Perego, C.; Carati, A.; Ingallina, P.; Mantegazza, M. A.; Bellussi, G. *Appl. Catal. A* **2001**, *221*, 63.
(22) Caruso, F. *Adv. Mater.* **2001**, *13*, 11.
(23) Lou, X. W.; Archer, L. A.; Yang, Z. *Adv. Mater.* **2008**, *20*, 3987.
(24) Chen, D.; Li, L. L.; Tang, F. Q.; Qi, S. *Adv. Mater.* **2009**, *21*, 3804.
(25) Lu, Y.; Yin, Y.; Li, Z.; Xia, Y. *Nano Lett.* **2002**, *2*, 785.
(26) Ma, D.; Veres, T.; Clime, L.; Normandin, F.; Guan, J.; Kingston, D.; Simard, B. *J. Phys. Chem. C* **2007**, *111*, 1999.
(27) Bouizi, Y.; Rouleau, L.; Valtchev, V. P. *Chem. Mater.* **2006**, *18*, 4959.
(28) Zhao, W.; Gu, J.; Zhang, L.; Chen, H.; Shi, J. *J. Am. Chem. Soc.* **2005**, *127*, 8916.
(29) Joo, S. H.; Park, J. Y.; Tsung, C. K.; Yamada, Y.; Yang, P.; Somorjai, G. A. *Nat. Mater.* **2009**, *8*, 126.
(30) Deng, Y.; Qi, D.; Deng, C.; Zhang, X.; Zhao, D. *J. Am. Chem. Soc.* **2008**, *130*, 28.
(31) Deng, Y.; Deng, C.; Qi, D.; Liu, C.; Liu, J.; Zhang, X.; Zhao, D. *Adv. Mater.* **2009**, *21*, 1377.
(32) Li, W.; Deng, Y.; Wu, Z.; Qian, X.; Yang, J.; Wang, Y.; Gu, D.; Zhang, F.; Tu, B.; Zhao, D. *J. Am. Chem. Soc.* **2011**, *133*, 15830.
(33) Liu, J.; Sun, Z.; Deng, Y.; Zou, Y.; Li, C.; Guo, X.; Xiong, L.; Gao, Y.; Li, F.; Zhao, D. *Angew. Chem. Int. Ed.* **2009**, *48*, 5875.
(34) Xu, L.; Ren, Y.; Wu, H.; Liu, Y.; Wang, Z.; Zhang, Y.; Xu, J.; Peng, H.; Wu, P. *J. Mater. Chem.* **2011**, *21*, 10852.
(35) Qian, X.; Li, B.; Hu, Y.; Niu, G.; Zhang, Y.; Che, R.; Tang, Y.; Su, D.; Asiri, A. M.; Zhao, D. *Chem.—Eur. J* **2012**, *18*, 931.
(36) Qian, X.; Du, J.; Li, B.; Si, M.; Yang, Y.; Hu, Y.; Niu, G.; Zhang, Y.; Xu, H.; Tu, B.; Tang, Y.; Zhao, D. *Chem. Sci.* **2011**, *2*, 2006.
(37) Peng, H.; Xu, L.; Wu, H.; Wang, Z.; Liu, Y.; Li, X.; He, M.; Wu, P. *Microporous Mesoporous Mater.* **2012**, *153*, 8.
(38) Song, F.; Liu, Y.; Wu, H.; He, M.; Wu, P.; Tatsumi, T. *J. Catal.* **2006**, *237*, 359.
(39) Zhao, S.; Xie, W.; Yang, J.; Liu, Y.; Zhang, Y.; Xu, B.; Jiang, J.; He, M.; Wu, P. *Appl. Catal. A* **2011**, *394*, 1.
(40) Wu, P.; Tatsumi, T.; Komatsu, T.; Yashima, T. *J. Phys. Chem. B* **2001**, *105*, 2897.
(41) Wu, P.; Tatsumi, T.; Komatsu, T.; Yashima, T. *Chem. Lett.* **2000**, 774.
(42) Chen, L.; Horiuchi, T.; Mori, T.; Maeda, K. *J. Phys. Chem. B* **1999**, *103*, 1216.
(43) Fan, W.; Wu, P.; Tatsumi, T. *J. Catal.* **2008**, *256*, 62.
(44) Stöber, W.; Fink, A.; Bohn, E. *J. Colliod. Inter. Sci.* **1968**, *26*, 62.
(45) Kresge, C. T.; Leonowicz, M. E.; Roth, W. J.; Vartuli, J. C.; Beck, J. S. *Nature* **1992**, *359*, 710.
(46) Zhao, D.; Feng, J.; Huo, Q.; Melosh, N.; Fredrickson, G. H.; Chmelka, B. F.; Stucky, G. D. *Science* **1998**, *279*, 548.
(47) Wu, P.; Ruan, J.; Wang, L.; Wu, L.; Wang, Y.; Liu, Y.; Fan, W.; He, M.; Terasaki, O.; Tatsumi, T. *J. Am. Chem. Soc.* **2008**, *130*, 8178.
(48) Oikawa, M.; Fukao, M. U.S. Patent 7067699, 2006.
(49) Petrini, G.; Cesana, A.; De Alberti, G.; Genoni, F.; Leofanti, G.; Padovan, M.; Paparatto, G.; Roffia, P. *Stud. Surf. Sci. Catal.* **1991**, *69*, 761.
(50) Mantegazza, M. A.; Cesana, A.; Pastori, M. In *Catalysis of Organic Reactions*;Malz, R.E., Ed.; Marcel Dekker, New York, 1996, 97.
(51) Mantegazza, M. A.; Cesana, A.; Pastori, M. *Top. Catal.* **1996**, *3*, 327.